Nature of Impurities in π-Conjugated Polymers Prepared by Ferric Chloride and Their Effect on the Electrical Properties of Metal–Insulator–Semiconductor Structures

Mohamed S. A. Abdou,[†] Xiaotang Lu,[⊥] Zi W. Xie,[§] Frank Orfino,[†] M. Jamal Deen,*[,‡] and Steven Holdcroft*[,†]

Department of Chemistry, Simon Fraser University, Burnaby, B.C., V5A 1S6 Canada, and School of Engineering Science, Simon Fraser University, Burnaby, B.C., V5A 1S6 Canada

Received July 19, 1994. Revised Manuscript Received January 20, 1995[⊗]

Poly(3-hexylthiophene), prepared by oxidative coupling using ferric chloride, has been purified to different extents so as to yield a series of samples with identical chemical structure and molecular weight but containing varying levels of residual iron impurity (0.05–3.2 wt % Fe). The polymers were analyzed by Mössbauer, UV–vis, IR, and EPR spectroscopies. The impurity is an octahedral iron(III) complex. The electrical response of thin polymer films was investigated in the form of metal–insulator–semiconductor (MIS) structures. Analysis of MIS field effect transistors (MISFETs) shows that both field effect mobility and bulk conductivity decrease as a function of impurity concentration. Capacitance–voltage (C–V) measurements performed on MIS structures show that the concentration of immobile, and ionized, electron-acceptor impurities increases with concentration of residual iron complexes. Evidence is provided for the formation of a relatively "thick" accumulation layer at the polymer/insulator interface. The thickness of the accumulation layer was found to be field dependent.

Introduction

The "neutral" form of π-conjugated polymers (<1 mol % doping level), such as polyacetylene, poly(vinylenephenylene), and polythiophene, has attracted considerable attention[1–4] due to delocalization of electrons which extends well beyond individual repeating units. Many of these polymers are processible and can be readily deposited onto substrates. In addition to the bulk electronic properties of the materials, the polymer/substrate interfacial region is under scrutiny because many potential applications employ thin polymeric films on substrates. The metal–insulator–semiconductor (MIS) structure is a useful device for studying interfacial properties, charge-carrier generation, and charge mobility. Several studies have been reported concerning polymer- and oligomer-based metal–insulator–semiconductor thin-film field effect transistors (MISFETs).[5–12] Of these, polythiophene-based structures have attracted the most attention.[7–11,13–17] The electronic properties of these polymers, as determined by electrical characterization of MIS structures is found to be highly dependent on the method of polymer preparation, the nature and level of impurities, and the thickness of the polymer film.

Polythiophenes and their derivatives have been prepared by three main methods, namely, electrochemical polymerization, Grignard polycondensation, and oxidative coupling using transition metal halides such as $FeCl_3$. Electrochemical polymerization is known to produce high purity polymers. This technique, however, can result in polymers with substantial chemical defects (i.e., α,α and α,β couplings) and very wide molecular weight distributions.[18,19] Typical electrical parameters of MISFETs based on polythiophene (PT) and poly(3-alkylthiophenes) (P3ATs) semiconductors prepared elec-

[†] Department of Chemistry.
[‡] School of Engineering Science.
[§] Present address: Intertech Systems Inc., Suite 438, 3700 Gilmore Way, Burnaby, B.C., Canada, V5G 4M1.
[⊥] Present address: Microtel Pacific Research, Burnaby, B.C., Canada, V5G 4M1.
* To whom correspondence should be addressed.
[⊗] Abstract published in *Advance ACS Abstracts,* March 1, 1995.

(1) Horowitz, G. *Adv. Mater.* **1990**, *2*, 287.
(2) Bradley, D. D. C. *Polym. Int.* **1991**, *26*, 3.
(3) Skotheim, B., Ed. *Handbook of Conducting Polymers*; Marcel Dekker: New York, 1986; Vol. 1, 2.
(4) Bredas, J. L.; Silbey, R., Eds. *Conjugated Polymers*; Kluwer Academic: Dordrecht, The Netherlands, 1991.
(5) Horowitz, G.; Fichou, D.; Peng, X.; Xu, Z.; Garnier, F. *Solid State Commun.* **1989**, *72*, 381.
(6) Garnier, F.; Horowitz, G.; Peng, X.; Fichou, D. *Adv. Mater.* **1990**, *2*, 592.
(7) Tsumura, A.; Koezuka, H.; Ando, T. *Appl. Phys. Lett.* **1986**, *49*, 1210.
(8) Tsumura, A.; Koezuka, H.; Ando, T. *Synth. Met.* **1988**, *25*, 11.
(9) Assadi, A.; Svensson, C.; Willander, M.; Inganas, O. *Appl. Phys. Lett.* **1988**, *53*, 195.
(10) Paloheimo, J.; Kuivalainen, P.; Stubb, H.; Vuorimaa, E.; Yli-Lahti, P. *Appl. Phys. Lett.* **1990**, *56*, 1157.
(11) (a) Xie, Z.; Abdou, M. S. A.; Lu, X.; Deen, M. J.; Holdcroft, S. *Can. J. Phys.* **1992**, *70*, 1171. (b) Abdou, M. S. A.; Xie, Z.; Deen, M. J.; Holdcroft, S. *Adv. Mater.*, in press.
(12) Burroughes, J. H.; Jones, C. A.; Friend, R. H. *Nature* **1988**, *335*, 137.
(13) Assadi, A.; Willander, M.; Svensson, C.; Helberg, J. *Synth. Met.* **1993**, *58*, 187.
(14) Dyreklev, P.; Inganas, O.; Paloheimo, J.; Stubb, H. *Synth. Met.* **1993**, *55–57*, 4139.
(15) Paloheimo, J.; Stubb, H.; Yli-Lahti, P.; Kuivalainen, P. *Synth. Met.* **1991**, *41–43*, 563.
(16) Dyreklev, P.; Gustaffsson, G.; Inganas, O.; Stubb, H. *Solid State Commun.* **1992**, *82*, 317.
(17) Taylor, D. M.; Gomes, H. L.; Underhill, A. E.; Edge, S.; Clemenson, P. I. *J. Phys. D: Appl. Phys.* **1991**, *24*, 2038.
(18) Sato, M.; Shimizu, T.; Yamauchi, A. *Makromol. Chem.* **1990**, *191*, 313.
(19) Hotta, S. *Synth. Met.* **1987**, *22*, 103.

0897-4756/95/2807-0631$09.00/0

Table 1. Effect of Synthetic Method on the Electrical Properties of Poly(3-alkylthiophenes)

electrical parameter	synthetic method: electrochemical polymerization	Grignard polycondensation	oxidative coupling
σ (S/cm)	5×10^{-8}	10^{-6}	10^{-7}
μ_{FET} (cm^2/V s)[a]	10^{-5}	$10^{-4}-10^{-5}$	$10^{-4}-10^{-5}$
n (cm^{-3})[b]	3×10^{16}[e]	3×10^{17}[e]	
g_m (S)[c]	3×10^{-9}		1×10^{-9}
V_{th} (V)[d]	−13		−1.0
impurity concn (cm^{-3})	ClO_4^-	I^-/I 10^{18}[f]	Fe(III) complex 5.1×10^{18}[g]
ref	7, 8, 17	9, 13−16	11, 24

[a] Field effect mobility. [b] Carrier concentration. [c] Transconductance. [d] Threshold voltage. [e] Estimated from $I-V$ characteristics of polymer-MISFETs using $\sigma = e\mu n$. [f] Determined by ESR and RBS (Rutherford backscattering). [g] Determined by atomic absorption.

trochemically are given in Table 1. Alternatively, the Grignard polycondensation is a versatile synthetic method for controlling the stereoregularity of the polymer.[20,21] The main disadvantages of this technique are lower molecular weights and high concentrations of residual impurities (i.e., iodide $\sim 10^{18}$ cm^{-3}).[15] Electrical parameters are reported in Table 1.

The oxidative coupling method produces polymers of much higher molecular weight (M_w up to 250 000) with a relatively high degree of stereoregularity (80% head-to-tail, 20% head-to-head) for P3ATs.[22,23] Resulting polymers contain residual iron(III) salts which can be reduced in concentration with rigorous purification.[24] Electrical parameters of devices constructed based on this polymer are reported in Table 1.

In addition to those described above, a number of studies have utilized FETs possessing novel device configurations. For example, Schottky gated FETs using free standing poly(3-alkylthiophene) films with Schottky gated electrode configurations have been reported.[13,25−27] Mobilities were estimated to be $\sim 10^{-3}-10^{-5}$ cm^2/V s. Nanotransistors and transistors fabricated on nanometer metal islands have also been investigated.[28,29] The field effect mobility of carriers (μ_{FET}) in these transistors was similar to microscale devices ($\sim 10^{-5}$ cm^2/V s). The effect of enhanced molecular order via stretch orientation and Langmuir−Blodgett (LB) techniques on device performance has also been investigated. Field effect mobilities, however, were similar to conventional polymer devices.[10,16] Spatial control of the electrical properties of P3ATs-based devices has also been investigated. Semiconducting π-conjugated polymer regions have been spatially converted to insulating regions by virtue of their photooxidative chemistry.[11,24] This concept was used to convert resistor-like characteristics of thick-film P3AT-MISFETs into devices possessing encapsulating insulating layers.

Thiophene oligomers (α-nT, $n = 3-8$) are particularly interesting because they serve as models of the parent polythiophene, and thin oligomeric films can be prepared in a much more ordered state.[5,6,30−43] Oligomers have the advantage of possessing well-defined structure and can be prepared as highly pure, crystalline solids with conductivities of $\sim 10^{-6}$ S/cm. This relatively high conductivity is attributed to the presence of bulk impurities which give rise to free charge carriers.[36] The field effect mobility and charge density of α-6T oligomer based-MISFETs are reported to be $\sim 10^{-4}-10^{-5}$ cm^2/V s and 10^{14} cm^{-3}, respectively.[5,6,41,43] The field effect mobility is found to be dependent on the nature of the insulating material used in the MIS device. Cyanoethylpullulane insulator-based devices ($\epsilon = 18.5$) yields μ_{FET} of 2×10^{-1} cm^2/V s, while SiO_2-based devices ($\epsilon = 3.9$) yield values of 5.0×10^{-5} cm^2/V s.[35−37] This difference is attributed to the influence of the insulator on the crystallinity of the oligomers at the semiconductor−insulator interface. Derivatization of thiophene oligomers is found to have a dramatic effect on μ_{FET}. Oligomers end-capped with alkyl groups have much higher field effect mobilities (1.5×10^{-2} cm^2/V s) by virtue of self-organization of the constituent molecules on the insulator.[39−42] Substitution at the β-position of thienyl moieties with alkyl groups, however, results in a substantial decrease in μ_{FET} (5×10^{-6} cm^2/V s).[38] An important consequence of the work on oligomers is the discovery that electronic conduction appears to be much faster in the direction of the π-stack.

Capacitance−voltage (C−V) measurements of MIS structures complement field effect transistor studies. For p-type semiconductors, ramping the bias from positive to negative voltage usually increases the overall capacitance of the structure, after which a constant capacitance is reached having a value equal to the geometric capacitance of the oxide layer. This behavior is typical of most polymer-MIS structures indicating that the conduction channel is due to accumulation of majority positive carriers at insulator/polymer interface. A depletion layer is formed under positive gate bias, but

(20) Mao, H.; Holdcroft, S. *Macromolecules* **1992**, *25*, 554.
(21) McCullough, R.; Lowe, R. D. *J. Chem. Soc., Chem. Commun.* **1992**, 70.
(22) Sugimoto, R.; Takeda, S.; Gu, H. B.; Yoshino, K. *Chem. Express* **1986**, *1*, 635.
(23) Sato, M.; Morii, H. *Macromolecules* **1991**, *24*, 1196.
(24) Abdou, M. S. A.; Holdcraft, S. *Macromolecules* **1993**, *26*, 2954.
(25) Ohmori, Y.; Takahashi, H.; Muro, K.; Uchida, M.; Kawai, T.; Yoshino, K. *J. Appl. Phys.* **1991**, *30*, L610.
(26) Ohmori, Y.; Takahashi, H.; Muro, K.; Uchida, M.; Kawai, T.; Yoshino, K. *J. Appl. Phys.* **1991**, *30*, L1247.
(27) Ohmori, Y.; Muro, K.; Yoshino, K. *Synth. Met.* **1993**, *55−57*, 4111.
(28) Paloheimo, J.; Franssila, S.; Kuivalainen, P.; Stubb, H. *Thin Solid Films* **1993**, *41−43*, 563.
(29) Paloheimo, J.; Stubb, H.; Gronberg, L. *Synth. Met.* **1993**, *55−57*, 4198.
(30) Garnier, F.; Horowitz, G. *Synth. Met.* **1987**, *18*, 693.
(31) Garnier, F.; Horowitz, G.; Fichou, D. *Synth. Met.* **1989**, *28*, 705.
(32) Fichou, D.; Horowitz, G.; Nishikitani, Y.; Garnier, F. *Synth. Met.* **1989**, *28*, 723.
(33) Horowitz, G.; Peng, X.; Fichou, D.; Garnier, F. *J. Appl. Phys.* **1990**, *67*, 528.
(34) Horowitz, G.; Peng, X.; Fichou, D.; Garnier, F. *J. Mol. Electron.* **1991**, *7*, 85.
(35) Garnier, F.; Horowitz, G.; Fichou, D. In *Electronic Properties of Polymers*; Kuzmany, H., Mehring, M., Roth, S., Eds.; Springer-Verlag: Berlin, 1992; p 458.
(36) Delannoy, Ph.; Horowitz, G. In *Electronic Properties of Polymers*; Kuzmany, H., Mehring, M., Roth, S., Eds.; Springer-Verlag: Berlin, 1992; p 466.
(37) Horowitz, G.; Peng, X.; Fichou, D.; Garnier, F. *Synth. Met.* **1992**, *51*, 419.
(38) Horowitz, G.; Deloffre, F.; Garnier, F.; Hajlaoui, R.; Hmyene, M.; Yassar, A. *Synth. Met.* **1993**, *54*, 435.
(39) Garnier, F.; Deloffre, F.; Horowitz, G.; Hajlaoui, R. *Synth. Met.* **1993**, *55−57*, 4747.
(40) Garnier, F.; Yassar, A.; Hajlaoui, R.; Horowitz, G.; Deloffre, F.; Servet, B.; Ries, S.; Alnot, P. *J. Am. Chem. Soc.* **1993**, *115*, 8716.
(41) Akimichi, H.; Waragai, K.; Hotta, S.; Kano, H.; Sakaki, H. *Appl. Phys. Lett.* **1991**, *58*, 1500.
(42) Waragai, K.; Akimichi, H.; Hotta, S.; Kano, H.; Sakaki, H. *Synth. Met.* **1993**, *55−57*, 4053.
(43) Ostoji, P.; Guerri, S.; Rossini, S.; Servidori, M.; Taliani, C.; Zamboni, R. *Synth. Met.* **1993**, *54*, 447.

no inversion of majority carriers has been observed for polythiophenes-based devices.[8,33] The C−V characteristics are qualitatively similar to metal−insulator-p-type silicon structures, which operate under the formation of an accumulation layer under negative bias. C−V investigations also provide information on the nature of polymer/metal interfaces and the dopant distribution profile.[44,45] Measurements on Al/polymer/Au and ITO/polymer/Au Schottky diodes show that the dopant is not homogeneously distributed in the polymer film but is concentrated at the polymer/metal interface. Furthermore, application of an electric field for prolonged periods (2 V back bias for 3.5 h) caused migration of dopant. It is important to note that the polymer used in the study was prepared by the Grignard route which produces highly mobile iodide impurities. Whether or not dopant diffusion is important in polymers which contain less mobile impurities, such as those obtained during the oxidative coupling, remains to be seen.

The parent π-conjugated polymer polyacetylene (PA) has also been actively studied as the semiconducting component in MISFETs.[12,46−48] The polymer is also a p-type semiconductor and the mobility of charge carriers is similar to that of other π-conjugated polymers (~10^{-5} cm^2/V s). The density of charge carriers, as calculated from measurements of depletion widths in Scottky barrier diodes, is calculated to be ~10^{16} cm^{-3}. Electron spin resonance (ESR) results show a rather high-spin concentration (10^{19} cm^{-3}). The origin of these carriers is attributed to defects and impurities associated with isomerization from cis to trans. It is concluded that dopants associated with the carriers do not readily migrate under an applied electric field as evidenced by C−V measurements.[47]

The work described above highlights the interesting electrical properties of π-conjugated polymers and the significant efforts that have been made to understand these properties. However, the origin of charge generation and charge migration is poorly understood. *Pure* conjugated polymers should be insulators (conductivity <10^{-9} S/cm) because of their wide bandgap. It is believed, but not proven, that unintentional doping of the material by residual catalyst used in the polymerization process leads to the formation of acceptor states in the bandgap and the semiconducting properties. Field effect transistors thus operate by controlling the space charge density, which modulates the conductance of the polymer film. It is not clear, however, whether the electric field applied across the gate and source generates new carriers or simply modulates the distribution of charge carriers already existing in the polymer. Voltage-modulated transmission measurements on transparent MIS structures have indeed revealed the formation of polaron-like states upon application of negative biases[49,50] which result in 5% bleaching in the luminescence signal.[14] The latter is readily explained by an increase in nonradiative recombination of singlet polaron-excitons at field-generated charged polaronic sites.

The work presented in this paper was prompted by a lack of understanding of the origin of charge carriers in polymer-MIS structures. In this study, electrical characteristics of poly(3-hexylthiophene) synthesized by chemical oxidative coupling using $FeCl_3$, have been investigated by chemical and spectroscopic analyses, electrical characterization of MISFETs, and C−V measurements on MIS structures. Three samples of poly(3-hexylthiophene) were investigated. The samples were chemically identical but differed in their relative concentration of residual iron impurity. Electrical parameters have been determined in order to examine the relationship between residual impurities, charge carriers and electronic properties of poly(3-alkylthiophenes).

Experimental Section

Polymer Synthesis and Purification. Polymerization of 3-hexylthiophene was achieved by chemical oxidative coupling according to the procedure described by Sugimoto et al.[22] The solid product was filtered and washed successively with ammonia solutions (28%), water, and finally acidified methanol. The crude polymer was dissolved in hot dichloromethane, and insoluble products were removed by filtration. The polymer was precipitated by adding methanol. The precipitate was filtered and dried under reduced pressure at 50 °C (P3HT-A). A fraction of the sample was purified further by Soxhlet extraction using methanol (2 days) and acetone (5 days) (P3HT-B). Subsequently, a fraction of this polymer was purified further by treating a solution of the polymer in $CHCl_3$ with aqueous ammonia solutions (28%). The polymer was precipitated, washed to chloride-free waste, and dried as described above (P3HT-C). By this route three polymer samples containing different levels of iron impurities were obtained. The number average molecular weight, M_n, was 8500 for all three samples and the molecular weight distribution (MWD) was ~3. The ratio of head-to-tail:head-to-head dyads was 80:20. λ_{max} was 435 nm (in $CHCl_3$).[51] Iron contents were determined by standard acid digestion procedures followed by atomic absorption spectroscopy.[52] P3HT-A contained 3.2 wt % (9.6 mol %) based on the ratio of Fe to thienyl rings; P3HT-B contained 1.32 wt % (4.15 mol %); and P3HT-C contained 0.05 wt % (0.15 mol %) of iron.

Instrumentation. Infrared spectra were recorded on a Bomem Michelson Model 120 FT-IR spectrometer. UV spectra were recorded on a Perkin-Elmer Lambda 3A and Cary E1 (Varian) spectrophotometer. The molecular weight of the synthesized polymers was measured by gel permeation chromatography (GPC) using 10^5−10^4- and 10^3-Å μ-Styragel columns at 25 °C. Polymers were eluted with tetrahydrofuran and detected using a UV−vis spectrophotometer (Waters 486) and a differential refractometer (Waters R401). Data were acquired, stored, and analyzed using an IBM personal computer and custom-written software. The concentration of iron was determined by atomic absorption spectroscopy using standard acid digestion procedures.[52] The measurements were carried out using a Perkin-Elmer 1100B AA spectrometer.

X-ray experiments were performed with a Siemens D-5000 diffractometer with a Cu Kα source and graphite monochromator. The samples had a thickness of 0.5−1.0 μm and a

(44) Gustafsson, G.; Sundberg, M.; Inganas, O.; Svensson, J. *J. Mol. Electron.* **1990**, *6*, 105.
(45) Gustafsson, G.; Inganas, O.; Sundberg, M.; Svensson, J. *Synth. Met.* **1991**, *41−43*, 499.
(46) Burroughes, J. H.; Jones, C. A.; Friend, R. H. *Synth. Met.* **1989**, *28*, C735.
(47) Friend, R. H.; Burroughes, J. H. *J. Chem. Soc., Faraday Discuss.* **1989**, *88*, 213.
(48) Burroughes, J. H.; Jones, C. A.; Lawrence, R. A.; Friend, R. H. In *Electronic Properties of Conjugated Polymers*; Kuzmany, H., Mehring, M., Roth, S., Eds.; Springer-Verlag: Berlin, 1989; p 437.
(49) Ziemelis, K. E.; Hussain, A. T.; Bradley, D. D. C.; Friend, R. H.; Ruhe, J.; Wegner, G. *Phys. Rev. Lett.* **1991**, *66*, 2231.
(50) Ziemelis, K. E.; Hussain, A. T.; Bradley, D. D. C.; Friend, R. H.; Ruhe, J.; Wegner, G. *Synth. Met.* **1991**, *41−43*, 1045.
(51) Patil, A. O.; Heeger, A. J.; Wudl, F. *Chem. Rev.* **1988**, *88*, 183.
(52) Quarmmby, C.; Grimshaw, H. M. *Analyst* **1967**, *92*, 305.

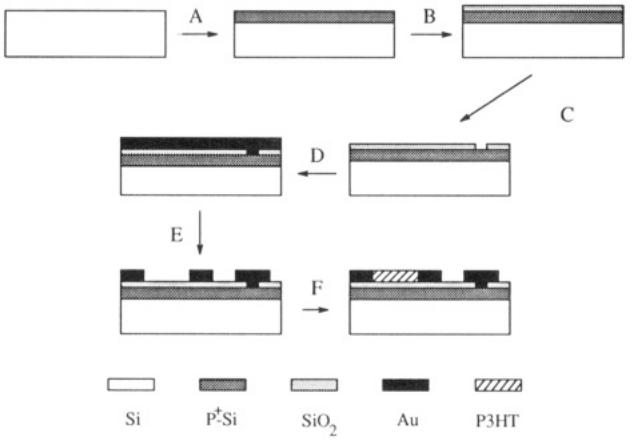

Figure 1. Fabrication scheme for polymer-MISFET.

geometry of 2 × 2 cm^2. Mössbauer spectra were recorded on a constant-acceleration Harwell Instruments spectrometer (200 series) with a $^{57}Co/Rh$ source (New England Nuclear). The 35.5 keV Mössbauer γ-ray was monitored through the 6 keV escape peak in a Xe/CO_2 proportional counter. The spectra were accumulated in a Nuclear Data 66 analyzer as 256-channel spectra and were subsequently computer-fitted to Lorentzian line shapes using an IBM 4341 mainframe computer. Absorbers, containing ca. 80 mg of polymer sample, were mounted in Teflon holders. The cross-sectional area of the sample was 2 cm^2. Measurements were carried out at 77 K. The isomer shifts are quoted with respect to iron metal.

Electron paramagnetic resonance (EPR) measurements were performed on polymer samples several micrometer thick using an X-band (9.5 GHz) Bruker ESC106 spectrometer at room temperature. Freshly recrystallized DPPH (α,α′-diphenyl-β-picrylhydrazyl) was used as the reference for g value and intensity calibration. The EPR line width for DPPH was ca. 1.5 G. The microwave power was set to well below the sample saturation level and the modulation amplitude was kept at ca. 25% of the peak-to-peak line width. Spectra were obtained at 25 °C and ambient pressure.

Fabrication and Analysis of MIS Devices. Silicon was chosen as the support substrate for the fabrication of polymer devices because it can be heavily doped to form a gate electrode and thermally oxidized to yield a silicon oxide insulating layer. The Si substrate plays no *active* role in the device operation. Two interdigital structures of gold were deposited photolithographically on top of the insulator and used as source and drain. The polymer semiconductor lyaer was spin cast onto the structure to form working devices. A detailed description of the fabrication process is given below and depicted in Figure 1: (A) The substrate was an oriented n/p-type silicon wafer. After performing standard degrease and clean procedures,[53] the dopant source (B-155 Allied-Signal Inc.) was spin cast onto the wafer. Thermal diffusion of dopants was carried out at 1100 °C under a N_2 atmosphere. The heavily doped layer served as a gate for the polymer-FET structure. (B) A layer of silicon oxide (200 nm) was grown by a combination of dry and wet oxidations procedures at 1100 °C.[53] (C) An AZ 1312SFD (Allied-Signal Inc.) photoresist was used to perform laser direct writing photolithography on the oxide layer in order to open connection windows. The procedure for photolithography was spin casting of the photoresist and baking at 95 °C for 0.5 h, exposure to 442 nm light, development using by an AZ developer (Shipley), and postbaking at 120 °C for 0.5 h. (D) Vacuum evaporation of gold (20 nm). (E) Photolithography using an AZ 1312SFD photoresist, etching of exposed gold, and patterning of 100 gold interdigitated fingers of width 10 μm and length 300 μm and spaced 14 μm apart. (F) Exposure of the active region by photolithography. Followed by spin-casting of dilute polymer solution (7000 rpm, film thickness = 0.25 μm) and lift off of the remaining photoresist. A schematic representation of the polymer-MISFET used in this study is shown in Figure 2.

(53) Helen, I. P. *Practical Integrated Circuit Fabrication*; ICE staff ed., 1982.

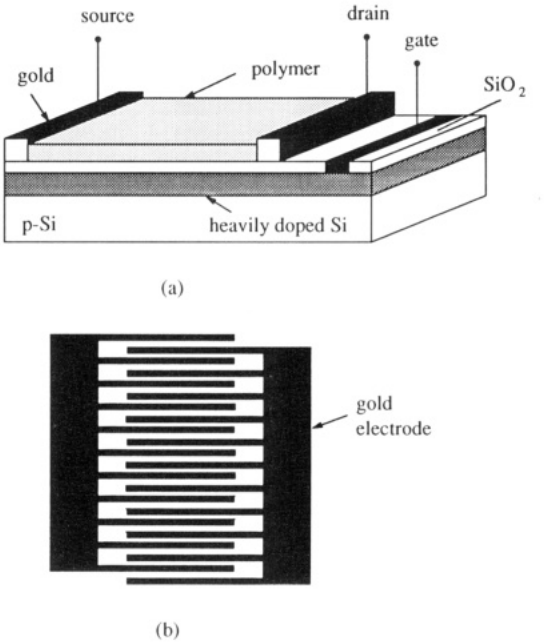

Figure 2. (a) Schematic representation of polymer-MISFET. (b) Pattern of source and drain contacts.

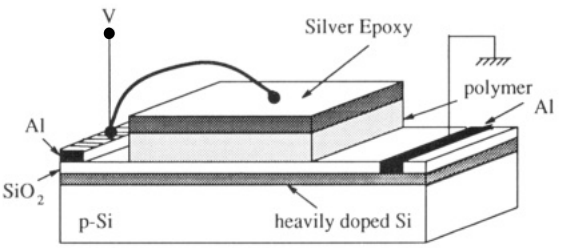

Figure 3. Polymer-MIS structure prepared for capacitance-voltage measurements.

MIS structures for capacitance−voltage measurements were also fabricated on a silicon wafer substrate, with silicon oxide as the insulator, and a heavily doped silicon layer acting as one of the electrodes. Aluminum was evaporated and patterned as contact pads, and polymer was spin-cast from solution (0.25 μm). Silver epoxy glue was applied to the top of polymer, and the structure was annealed in N_2 at 120 °C for 1 h. This structure is shown in Figure 3. The electrical contacts with the polymer were ohmic. The use of silver epoxy was preferred over metal evaporation in order to prevent exposure of the polymer to high temperature. This structure was bonded to a dual in-line package (DIP) and plugged into a HP 16058 test fixture with electrical and magnetic radiation shielding. C−V measurements were performed in a dark environment.

Current−voltage characteristics of polymer MISFETs were measured with a semiconductor parameter analyzer HP4145 and a Bausch and Lomb wafer probing station. Drain current was measured at different drain-source voltages ($I_{ds}-V_{ds}$) to observe polymer FET-like characteristics, while plots of drain current versus gate voltage ($I_{ds}-V_{gs}$) were constructed to determine the gate bias modulation of the FET conductive channel. Drain current-gate voltage measurements at the gate ($I_{gs}-V_{gs}$) provided information on the quality of the silicon oxide layer. Capacitance−voltage (C−V) characteristics were measured with Keithly 590 series CV meter. The voltage sweep was varied from −20 to 20 V at a sweep rate of 2 V/min. The ac frequency was 1 MHz. Electrical measurements were performed immediately following annealing in order to ensure the effect of oxygen on the electrical response was minimal.

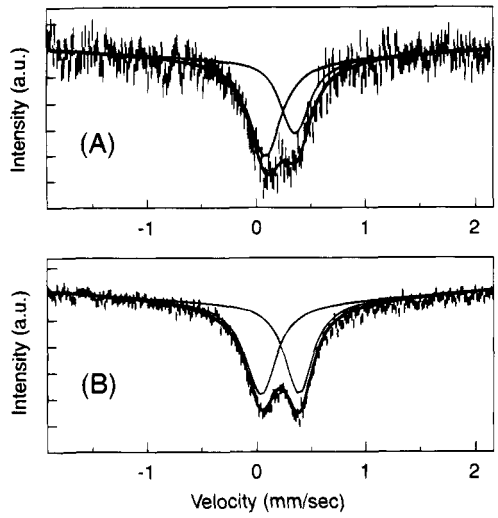

Figure 4. Mössbauer spectra of P3HT-C: (A) oxidized polymer; (B) neutral polymer. Solid lines represent Lorentzian fits to data.

Results

Chemical Characterization of Impurities. P3HT was prepared by oxidative coupling using $FeCl_3$ according to[22]

$$n(3HT) + 4nFeCl_3 \rightarrow Poly[(3HT)_n^{2+} \cdot 2nFeCl_4^-] + 2nFeCl_2 \quad (1)$$

The polymer is prepared in the oxidized form and requires reduction to the neutral, soluble form for polymer processing. Ammonia solutions were used to carry out the reduction according to reaction 2.[54]

$$3Poly[(3HT)_n^{2+}] + 8nNH_3 \xrightarrow{H_2O} 3P3HT + nN_2 + 6nNH_4^+ \quad (2)$$

As described in the Experimental Section, the purification of polymer was performed to varying degrees so as to produce three samples of polymer containing different levels of impurity. This ensures that the polymer's structure and molecular weight were identical and that variation in electrical properties originated only from the difference in impurity concentration. Atomic absorption spectroscopic analysis indicated the concentrations of residual iron were 0.05 wt % (P3HT-C), 1.3 wt % (P3HT-B), and 3.2 wt % iron (P3HT-A). Elemental analysis determined that the molar ratio of Fe:Cl was 1:1 for each polymer. Mössbauer spectroscopy was performed to provide further information on the nature of the iron impurities. Figure 4 shows the Mössbauer spectra of P3HT-C. The isomer shift, δ, and the quadrupole splitting, Δ, of the neutral polymer (Figure 4B) are 0.26 and 0.32 mm s^{-1} respectively; indicative of an iron(III) octahedral complex.[55] P3HT-A and P3HT-B provided similar Mössbauer spectra, confirming the common nature of the iron complex in each of the samples. FTIR studies of neutralized P3HT reveal the absence of characteristic NH_4^+ absorptions

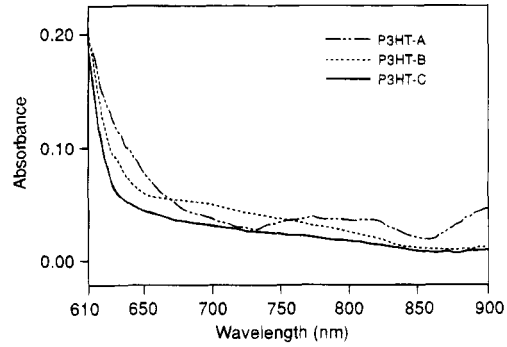

Figure 5. Effect of residual iron concentration on the electronic absorption tail of P3HT.

(3310, 3100, and 1080 cm^{-1}), indicating that NH_4^+ is not a constituent of either the iron complex or the polymer. FTIR of the polymer yields a broad absorption at 3500 cm^{-1} which is assigned to hydroxyl groups. The intensity of the absorption is dependent on the concentration of iron impurities indicating that OH groups are associated with the octahedral iron(III) complex and not the polymer.

(P3HT-A), (P3HT-B), and (P3HT-C) exhibit similar absorption spectra in the UV–vis region, but small perturbations are observed in the vis–NIR region which depend on the concentration of iron impurities. These perturbations are shown in Figure 5. For each of these films the thicknesses and optical densities at maximum absorbance were similar. The polymers show weak, broad transitions in 650–900 nm region which are interpreted as being due to the presence of low concentrations of (bi)polarons. These transitions become more pronounced with increasing iron concentration. There is some evidence that polaron formation is preferred with lower impurity concentrations, while bipolaron formation is more favored at higher concentrations.[50] This would be consistent with the fact that the bipolaron is thermodynamically more stable than two polarons so that coalescence of polarons occurs at higher concentrations. However, the lack of clearly defined absorption bands in this region and the presence of a strong π–π^* transition indicates that the polaron and bipolaron concentrations are very low.

EPR Analysis. EPR analysis of the polymers gave rise to a several characteristic signals. Dominant signals were observed for Fe^{3+} ($g = 2.02$).[56] The peak-to-peak line widths for its signal varied from 560 G for P3HT-C (0.05 wt % Fe) to 410 G for P3HT-A (3.2 wt % Fe). The line shapes exhibited a Lorentzian character which indicates relatively fast spin–lattice relaxation times. The doubly integrated intensity of the Fe^{3+} dispersion curves increased with increasing impurity content as expected.

Centered at 3350 G and superimposed on the broad Fe^{3+} signal was a much narrower dispersion curve which was intrinsic to the polymer. These signals are shown in Figure 6, and the extracted data presented in Table 2 for (P3HT-A), (P3HT-B), and (P3HT-C). The signal for P3HT-C has a g value of 2.0032, a line width of 6.00 G, a Gaussian line shape, and a spin density of

(54) Foot, P.; Ritchie, T.; Mohammed, F. *J. Chem. Soc., Chem. Commun.* **1988**, 1536.
(55) Greenwood, N. N.; Gibb, T. C. *Mössbauer Spectroscopy*; Chapman and Hall: London, 1971.
(56) (a) Wertz, J. E.; Bolton, J. R. *Electron Spin Resonance, Elementary Theory and Practical Applications*; McGraw-Hill: New York, 1972. (b) Zucharski, Z.; Winkler, H.; Trautwein, A. X.; Budrowski, C.; Butzlaff, C.; Length, M. *Hyperfine Interactions* **1991**, *69*, 659.

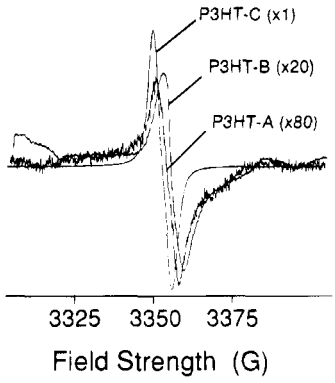

Figure 6. EPR spectra of P3HT containing different level of iron impurities: (A) P3HT-A, (B) P3HT-B, (C) P3HT-C.

Table 2. EPR Data for Poly(3-hexylthiophenes)

polymer	Fe content (wt %)	polymer[a] (10^{16} spins/g)	g value	ΔH_{p-p} (G)	line shape
P3HT-A	3.20	7.6	2.0029	6.43	Lorentzian
P3HT-B	1.32	4.6	2.0028	7.58	Gaussian
P3HT-C	0.05	127.4	2.0032	6.00	Gaussian

[a] These values are accurate to 15%.

1.3×10^{18} spins/g which indicates 1 spin/2820 thienyl rings. These parameters are consistent with values found in the literature.[57] The g value is similar to the free electron value of 2.00232[58] indicating localization of the electron on the polymer backbone rather than on the sulfur heteroatom.[59] For the high iron impurity level sample (3.2 wt % Fe) the spin density decreases to 7.6×10^{16} spins/g revealing a correlation between the impurity concentration and the number of unpaired electrons in the polymer. A similar decrease in spin density has been noted for polythiophene[59] and poly(3-hexylthiophene)[57] doped electrochemically with BF_4^- at high doping levels. A decrease in the g value, as well as a line-type change from Gaussian to Lorentzian, is reported, concluding that the observed EPR signal is due to delocalized spins.

Annealing of Polymer-MISFETs. It has been found that annealing of polymer-MISFETs under N_2 atmosphere at 180 °C was necessary to achieve a FET-like response for electrical characterization.[11,33] To explain the annealing effect, we note that spin coating alone often renders polymer films with a large free volume (~15%) and retention of 10–20% solvent.[60] Annealing above the glass transition or melting point of the polymer can help in reducing the free volume and trapped solvent thus leading to more compact and ordered films. The melting point of the polymer was determined by differential scanning calorimetry (DSC) to be 175 °C (Figure 7).[61,62] Following annealing at 180 °C in N_2, the chemical structure of the polymers as determined by FTIR did not change. The polymer does however undergo a thermal degradation process under O_2 at this temperature so that rigorous exclusion of oxygen is necessary during annealing. Details of this thermal oxidation process will be published separately.

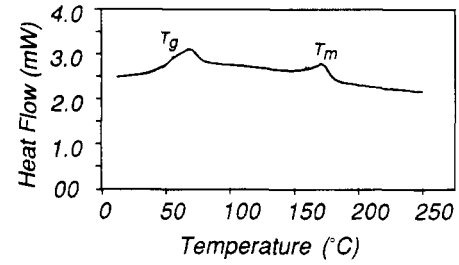

Figure 7. DSC thermogram of P3HT-C.

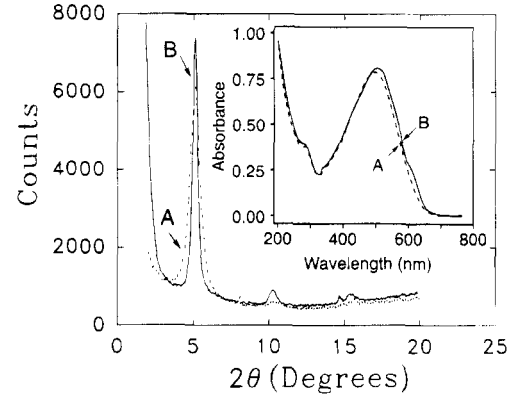

Figure 8. X-ray diffraction profiles of P3HT-C before (A) and after (B) annealing. Inset: Comparison of UV–vis absorption spectra of P3HT-C before (A) and after (B) annealing.

As anticipated, the concentrations of residual iron in the polymers were unchanged by the annealing process. Mössbauer spectroscopy on annealed samples revealed isomer shifts and quadrupole splittings which were identical to unannealed samples (i.e., 0.26 and 0.32 mm s^{-1}, respectively) indicating that the Fe impurity took the form of an iron(III) octahedral complex. FTIR of annealed P3HT exhibited a broad absorption at 3500 cm^{-1} even after annealing which indicated the persistence of hydroxyl groups. In addition, the strength of this absorption was proportional to Fe concentration thus the O–H groups appear to be associated with the Fe(III) complex. The molar ratio of Fe:Cl was not determined for annealed samples.

EPR analysis of annealed polymers indicated that annealing reduced the number of unpaired spins by 25–45% compared to unannealed samples. g values, peak-to-peak line widths, were virtually unchanged compared to unannealed samples. Dominant signals were also observed for Fe^{3+} (g = 2.02). The decrease in spin density with annealing is attributed to two factors: (1) an increase in crystallinity of the sample and hence more efficient coupling of spin centers (polarons) to form spinless bipolarons; (2) elimination of oxygen which forms a weak charge-transfer complex with oxygen.[11b]

The physical properties of the polymer were affected by annealing. X-ray diffraction analysis of thin films shows that the reflection signals are narrower and more pronounced for annealed films indicating an increase in crystallinity of the polymer (Figure 8). This has been recently reported for an analogous polymer, poly(3′,4′-

(57) (a) Onoda, M.; Manda, Y.; Morita, S.; Yoshino, K. *Jpn. J. Appl. Phys.* **1992**, *31*, 2265. (b) Inoue, M.; Inoue, M. B.; Castillo-Ortega, M. A. M. *Synth. Met.* **1989**, *33*, 355. (c) Vardeny, Z.; Ehrenfreund, E.; Brafman, O.; Nowak, M.; Schaffer, H.; Heeger, A. J.; Wudl, *Phys. Rev. Lett.* *56*, **1986**, 671. (d) Colaneri, N., Nowak, D., Spiegel, D., Hotta, S., Heeger, A. J. *Phys. Rev. B* **1987**, *36*, 7964.
(58) Wilkinson, D. T.; Crane, H. R. *Phys. Rev.* **1963**, *130*, 852.
(59) (a) Kaneto, K.; Hayashi, S.; Ura, S.; Yoshino, K. *J. Phys. Soc. Jpn.* **1985**, *54*, 1146. (b) Tanaka, K.; Shichiri, T.; Yoshizawa, K.; Yamabe, T.; Hotta, S.; Shimotsuma, W.; Yamauchi, J.; Deguchi, Y. *Solid State Commun.* **1984**, *51*, 565.
(60) Nalamasu, O., Ed. *Adv. Resist Technol. Process. XI, SPIE* **1994**, *2195*, 14.
(61) Chen, S.; Ni, J. *Macromolecules* **1992**, *25*, 6081.
(62) Tashiro, K.; Ono, K. K.; Minagawa, Y.; Kobayashi, M.; Kawai, T.; Yoshino, K. *J. Polym. Sci., Polym. Phys.* **1991**, *29*, 1223.

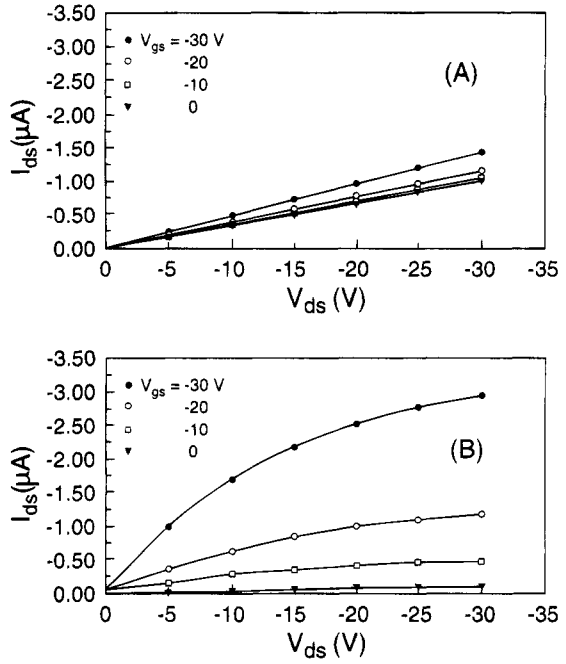

Figure 9. $I_{ds}-V_{ds}$ characteristics of (P3HT-C)-MISFET (Fe content = 0.05 wt %): (A) before annealing; (B) after annealing.

dibutyl-2,2′:5′2″-terthiophene).[63] UV–vis absorption spectroscopy shows a red shift in the absorption edge upon annealing (Figure 8, inset) attributed to a decrease in the bandgap energy due to increased π-interaction. Annealing therefore results in an enhancement of molecular order and π-interaction.

Polymer-MISFET *I–V* Characteristics. Prior to thermal annealing at 180 °C under a N_2 atmosphere, $I_{ds}-V_{ds}$ curves of polymer-MISFETs showed a large resistive current, a small gate bias modulation, and the absence of a saturation region (Figure 9A).

Figure 9B shows typical $I_{ds}-V_{ds}$ curves for an annealed (P3HT-C)-MISFET (0.05 wt % Fe). FET-like behavior is observed with typical linear and saturation regions.

The total current of a polymer MISFET can be separated into two components: channel current (I_{ch}) and bulk current (I_{bk}) ($I_{total} = I_{ch} + I_{bk}$). Using established MOSFET and semiconductor current–voltage relationships, the channel current, can be formulated as[64]

$$I_{ch} = \mu_{FET} C_{ox} \frac{W}{L}\left\{(V_{gs} - V_{th})V_{ds} - \frac{1}{2}V_{ds}^2\right\} \quad (3)$$

$$I_{ch} = \frac{1}{2}\mu_{FET} C_{ox} \frac{W}{L}(V_{gs} - V_{th})^2(1 + \lambda V_{ds}) \quad (4)$$

for linear and saturation operation modes respectively, where L and W are channel length and width, respectively, C_{ox} is capacitance of oxide layer, V_{gs}, V_{ds}, and V_{th} are gate, drain, and threshold voltages, respectively, and λ is the channel length modulation coefficient. The bulk current can be represented as

$$I_{bk} = \sigma \frac{W}{L} d_p V_{ds} \quad (5)$$

where d_p and σ are thickness and bulk conductivity of the polymer film.

The bulk conductivity can be determined from plots of $I_{ds}-V_{ds}$ at zero bias (eq 5). The bulk current is subtracted from drain currents (I_{ds}) at negative biases to determine the FET-like channel currents. Mobilities are determined using conventional MOS parameter extraction methods.[64] The field effect mobility of poly(3-hexylthiophene) was determined to be 2.3×10^{-5} cm^2/V s from data presented in Figure 9B. This is consistent with other reports.[13–17] In comparison with other polythiophenes, the mobility is higher than 3-octyl and 3-dodecyl derivatives $10^{-6}-10^{-7}$ cm^2/V s[15] but lower than 3-methyl- and 3-butyl-substituted analogues $10^{-3}-10^{-4}$ cm^2/V s.[17]

$I_{ds}-V_{gs}$ responses at different V_{ds} are shown in Figure 10. At zero gate bias, I_{ds} has a small current value, this is the bulk current at zero gate bias. For a small gate bias, I_{ds} increases linearly with V_{gs}. As V_{gs} is made more negative (−20 → −40 V), I_{ds} shows a sharp increase, which corresponds to large gate bias modulation in the saturation region. At even higher gate biases (>−50 V), the current increment decreases. This is presumably due to the increased carrier concentration at the polymer/insulator interface and subsequent surface scattering of the carriers.

Figure 10 can be replotted as $\sqrt{I_{ds}}$ versus V_{gs} at $V_{ds} = V_{gs}$ (Figure 11). At this bias the MISFET operates in the saturation region. From the intercept of this plot with voltage axis, a threshold voltage of −7.1 V was obtained, and from its gradient a mobility of 6.9×10^{-5} cm^2/V s was calculated. In subsequent analyses we found it more reliable to extract values of mobility from the linear region of the $I-V$ plot.

Effect of Impurity Concentration on Electrical Properties of Polymer MISFETs. Poly(3-alkylthiophenes) are p-type semiconductors. A possible source for extrinsic doping is residues remaining from use of polymerization catalyst. To investigate the role of residual catalyst on FET characteristics, poly(3-hexylthiophene) samples were prepared with varying levels of residual impurities. Figure 12 shows $I_{ds}-V_{ds}$ curves of MISFETs based on polymers (P3HT-A) and (P3HT-B). When these figures are compared with Figure 9B (P3HT-C), the former can be observed to possess more resistive character and a lesser field effect response. Values of mobility and conductivity for the polymer-MISFET were extracted from $I_{ds}-V_{ds}$ characteristics and are given in Table 3 together with values of σ. As the external impurity concentration increases, the bulk current and the field effect mobility decrease. These results verify that impurities play an important role in carrier transport.

C–V Characteristics for Polymer-Based MIS Structures. The capacitance of polymer-MIS structures were analyzed under high frequency (1 MHz). The dc voltage was ramped from −20 to 20 V at a rate of 2 V/min. A high frequency and slow sweep rate were chosen to exclude effects of both long relaxation times and the influence of mobile elements associated with the polymer. The equivalent circuit of the polymer-MIS structure is shown in Figure 13. The MIS structure can

(63) Wang, C.; Benz, M. E.; LeGoff, E.; Schindler, J. L.; Thomas, J. A.; Kannewurf, C. R.; Kanatzidis, M. G. *Chem. Mater.* **1994**, *6*, 401.
(64) Sze, S. M. *Physics of Semiconductor Devices*, 2nd., ed.; Wiley: New York, 1981.
(65) Nicollian, E. H.; Brews, J. R. *MOS Physics and Technology*; Wiley: New York, 1982.

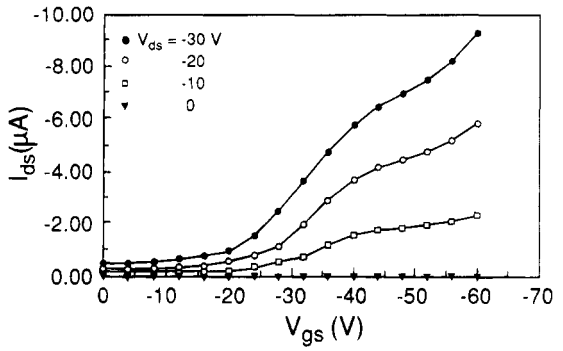

Figure 10. $I_{ds}-V_{gs}$ responses at different V_{ds} for annealed polymer-MISFET. Data extracted from Figure 9.

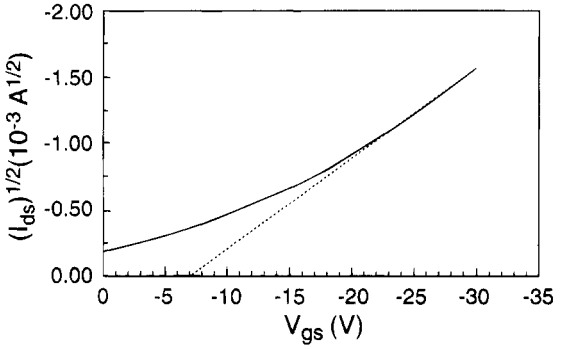

Figure 11. $\sqrt{I_{ds}}$ versus V_{gs} at $V_{ds} = V_{gs}$ for annealed polymer-MISFET. Data taken from Figure 9.

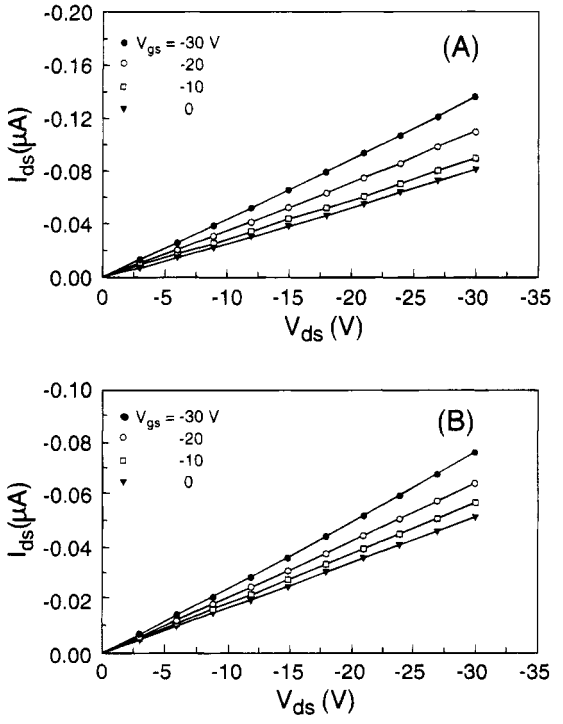

Figure 12. $I_{ds}-V_{ds}$ curves of annealed MISFETs based on polymers with iron contents of (A) 3.2 wt % (P3HT-A) and (B) 1.32 wt % (P3HT-B).

be considered to be a series circuit consisting of the insulator capacitance C_i and the semiconductor impedance (including semiconductor capacitance C_s, conductance G_s, and series resistance R_s). Series resistances associated with the thick polymer film ranged from 30 to 100 kΩ, and were compensated for the $C-V$ measurements. The relationship between series-resistance-compensated capacitance, C_c, with the measured capacitance, C_M, and measured conductance, G_M is given by

$$G_c = \frac{(G_M^2 + \omega^2 C_M^2)C_M}{a + \omega^2 C_M^2} \tag{6}$$

where

$$a = G_M - (G_M^2 + \omega^2 C_M^2)R_S$$

Figure 14 shows the C_c-V responses for polymer devices at 1 MHz for relatively thick films (~1 μm) of (P3HT-A), (P3HT-B), and (P3HT-C). The capacitance decreases when the applied voltage is made positive. No obvious minimum capacitance is observed for a high positive voltage. This indicates the absence of an inversion layer. No inversion layer has ever been observed in polythiophene MIS structures. Its absence is presumably due to a combination of difficulty in generating stable negatively charged carriers in the depletion region, and their very low rate of migration. The C−V characteristics are similar to silicon-based MIS diodes under deep depletion conditions.

The variation of capacitance in the deep depletion regime can be modeled as[65]

$$\left(\frac{C_i}{C_c}\right)^2 - 1 = \left(\frac{C_i}{A}\right)^2 \frac{2(V - V_f)}{qN_A\epsilon\epsilon_0} \tag{7}$$

where A is polymer-MIS diode area, N_A is the number of electron accepting impurities which give rise to charge

Table 3. Field Effect Mobilities, Conductivities, and Acceptor Concentrations of P3HT

polymer	Fe content wt % (cm^{-3})[a]	μ_{FET} ($cm^2/V\ s$)[b]	σ (S/cm)[b]	N_A (cm^{-3})[c]
P3HT-A	3.2 (3.9×10^{20})	6.4×10^{-8}	3.7×10^{-9}	5.8×10^{17}
P3HT-B	1.32 (1.7×10^{20})	8.4×10^{-7}	1.4×10^{-8}	1.7×10^{17}
P3HT-C	0.05 (5.9×10^{18})	2.3×10^{-5}	1.2×10^{-7}	5.1×10^{16}

[a] Determined by atomic absorption. [b] Determined by analysis of polymer FETs. [c] Determined by C−V measurements.

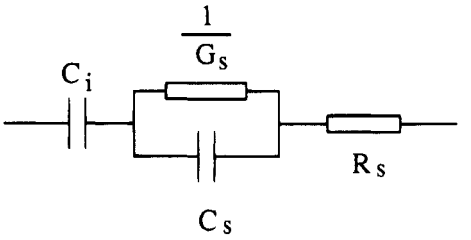

Figure 13. Equivalent circuit of polymer-MIS structure.

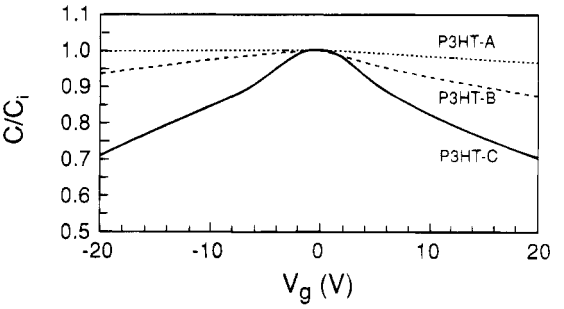

Figure 14. Capacitance−voltage characteristics of polymer-MIS structures: (A) P3HT-A; (B) P3HT-B; (C) P3HT-C. C is the overall capacitance of the MIS structure, C_i is the insulator (oxide) capacitance.

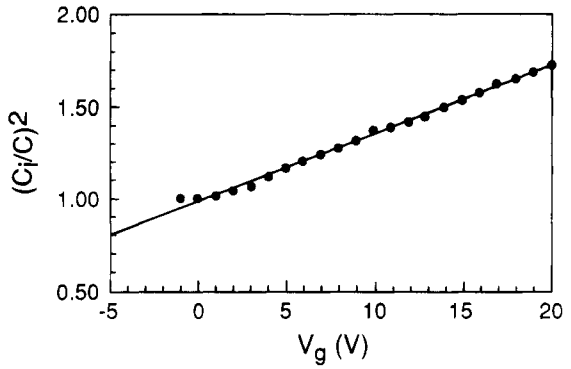

Figure 15. $(C_i/C)^2$ versus gate bias of (P3HT-C)-MIS diode.

carriers (majority carrier concentration), C_i is insulator capacitance, V is the applied voltage, V_f is the flat-band potential, and ϵ and ϵ_0 are the dielectric constants of the polymer and insulator, respectively. Values for N_A of 5.44×10^{17}, 1.54×10^{17}, and 4.7×10^{16} cm^{-3} were estimated from the slope of plots of $(C_i/C)^2$ against voltage for polymers P3HT-A, P3HT-B, and P3HT-C (Figure 15). Thus N_A increases with impurity (Fe complex) concentration. Upon closer inspection of the relationship between impurity concentration and carrier concentration, we note that the latter is orders of magnitude smaller. For example, the Fe impurity content was determined to be 5.9×10^{18} cm^{-3} for P3HT-C, whereas N_A was measured to be 5.1×10^{16} cm^{-3}. Clearly not all iron species take the form of electron-accepting impurities.

Under negative bias, it is reported that the capacitance of polymer-based FETs is independent of the voltage and that the capacitance of the structure is approximately equal to the geometric capacitance of the insulator, C_i.[8,12,33] This suggests that the accumulation layer has a very high differential capacitance due to its very thin nature. However, $C-V$ measurements performed in this study indicate that the capacitance decreases when the voltage is swept negatively, particularly for samples with low impurity levels. We conclude that the accumulation layer for the polymer-MIS structure is sufficiently thick to affect the total capacitance of the MIS structure. This is the first evidence of a relatively "thick" accumulation layer, and we attribute it to the low levels of residual impurities. It should be noted that, to our knowledge, $C-V$ measurements on other π-conjugated polymers have not evidenced such a thick accumulation layer and that this observation might be inherent to the P3ATs-Fe impurity systems.

The capacitance of the MIS structures at negative gate bias can be treated as an insulator capacitance, C_i, in series with accumulation layer capacitance, C_a. C_a can be represented as

$$C_a = \epsilon A/d_a \tag{8}$$

where ϵ is the dielectric constant of the polymer, A is the effective area of the MIS structure, and d_a is the bias-dependent accumulation layer thickness. The latter increases with the applied negative gate bias, and the capacitance subsequently decreases. The overall capacitance of the MIS structure, C_c, is given by

$$C_c = \frac{C_i C_a}{C_i + C_a} \tag{9}$$

where C_c is the series-resistance-compensated capacitance as described previously. This shows that C_c is expected to decrease as the accumulation layer capacitance decreases. The accumulation layer thickness were calculated as a function of applied gate biases for P3HT-C and are shown in Figure 16.

Discussion

Chemical characterization of these polymers reveals that the iron impurities exist in the form of an iron(III) octahedral complex. For unannealed samples, the chloride to iron ratio is 1:1. For complete compensation of charge the Fe complex requires two other anions. Given that purification was performed using ammonia solutions it is reasonable to assume these as hydroxyl groups. Retention of Cl was not determined for annealed samples. Nevertheless, Mössbauer spectroscopy indicates an octahedral complex for both annealed and unannealed samples so that additional molecules must be coordinated to Fe^{3+}. FTIR analyses indeed supports the presence of OH functionality although they cannot be specifically assigned to the Fe(III) complex. The possibility exists that the complex is coordinated to the polymer backbone.[66,67] Two main sites are available for coordination: π (η^5) coordination and S-bonded (η^1). Thus charge transfer between the conjugated polymer and the Fe^{3+} complex, as shown in Figure 17, might possibly be the origin of charge carriers. The equilibrium shown in Figure 17 must lie heavily to the left because (1) the concentration of carriers is orders of magnitude lower than the concentration of impurities and (2) the iron species are known to be overwhelmingly in the form of Fe(III).

Insight into the origin of charge carriers in semiconducting π-conjugated polymers has been provided by electrooptical measurements on polymer-MIS structures in which modulation of the optical transmission through the active polymer layer is observed as a function of bias voltage, i.e., voltage-modulated transmission (VMT).[49,50] The study revealed the presence of polaron and bipolaron states only upon application of a negative bias across polymer-MIS structures. Furthermore, the formation of these charged species was confirmed by voltage modulated photoluminescence for which application of a negative bias resulted in a 5% decrease in luminescence. Field-induced quenching of luminescence was attributed to nonradiative recombination of singlet polaron–excitons at charged polaronic sites. Both these studies indicate that localized charged states were largely absent in the absence of an applied field and were subsequently generated by the electric field.

This information is useful in interpreting the results in the present study regarding the origin of charge carriers and the field effect response of MIS structures. In the absence of an applied field transverse to the polymer film, the positive charge carriers originating from charge transfer between the polymer and Fe(III) impurities are distributed homogeneously throughout

(66) Angelici, R. J. *Coord. Chem. Rev.* **1990**, *105*, 61.
(67) Pannel, K. H.; Kalsotra, B. L.; Parkanyi, C. *J. Heterocycl. Chem.* **1978**, *15*, 1057.

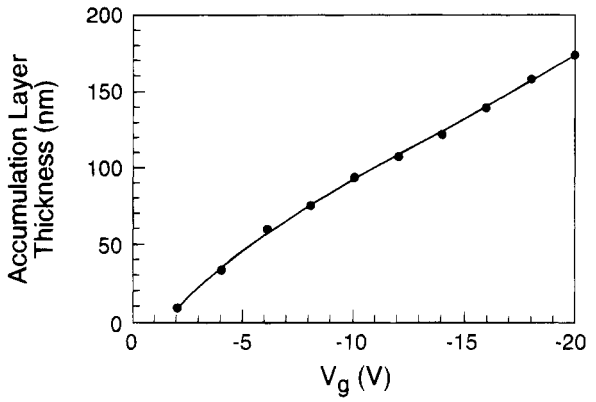

Figure 16. Accumulation layer thickness versus gate bias for (P3HT-C)-MIS diode.

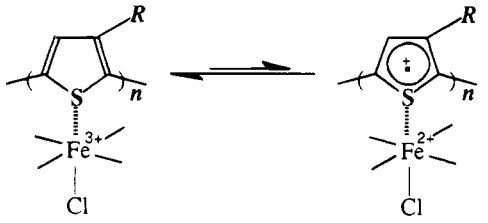

Figure 17. Scheme illustrating possible charge transfer between P3HT and residual Fe^{3+} impurities.

the polymer film. Thus for *unannealed* polymers P3HT-A, P3HT-B, and P3HT-C there exists a polaron for every 80 000, 3000, and 1250 thienyl rings, respectively. For annealed sampled of P3HT-A and P3HT-C one polaron exists for every 100 000 and 1810 rings, respectively. The relative concentration of bipolaronic species is unknown, but for the latter, the dominant charged species are polarons. The apparently low concentration of carriers barely perturbs the electronic structure of the π-system and thus the $\pi-\pi^*$ transition energy appears to be independent of impurity concentration; although weak transitions are observed in the region of 700–900 nm where polaron and bipolaron excitations are usually observed (Figure 5). Upon application of the electric field across a MIS structure, the positive charges are redistributed, and accumulated at the polymer/insulator interface so that an individual positive charge is distributed over only a relatively few thiophene rings. The accumulated charge takes the form of (bi)polarons which can be observed by optical spectroscopy.[49,50] It is not clear, however, whether the electric field increases the conductance of the polymer film in polymer-MISFETs because "trapped" charge carriers become available for conduction[68] or whether accumulation of charges increases the mobility of the carriers in the field effect channel.[69] Further work is required to clarify these mechanisms. In contrast to a previous study of polythiophene, we found no evidence for migration of impurities leading to their redistribution/accumulation under an applied field. This might be due to the bulkiness, and therefore slow migration, of the octahedral Fe complex. In the study, where impurity migration was observed, the polymer was prepared by the Grignard route for which impurities are mobile iodide species.

EPR spectroscopy has been used to provide information on the presence of charge carriers which possess spin, i.e., polarons. Previous studies correlating spin concentration with the level of doping (achieved electrochemically) show that the former decreases as the doping level is increased due to coalescence of polarons into spinless bipolarons. Ambiguity arises as to what level of doping is required to observe this decrease. A study on poly(3-methylthiophene) provides evidence that the spin concentration is maximum at 0.2 mol % doping (1 spin/500 thienyl rings).[57] Whereas studies from another group places this transion at 3 and 16 mol % for polythiophene and poly(3-hexylthiophene), respectively.[57a,59a] In our studies, in which the dopant is an impurity, the polaron concentration is observed to drop by a factor of 25 as the iron impurity concentration is increased. Simultaneously, the effective carrier concentration is apparently increasing as inferred from electrical characterization. Both these phenomena can be explained on the basis of coelescence of polarons into bipolarons. However, UV–vis data indicate only a small increase in bipolaron content as the impurity concentration is increased which implies the levels of doping are relatively low, consistent with one of the previous studies mentioned. If a much higher doping/impurity level was necessary to observe a decrease in spin concentration then this would be reflected in strong polaron and bipolaron excitations in the vis–NIR region, but this was not the case. In the case where the spin concentration falls below 0.2 mol % doping, the concentration of polarons and bipolarons and thus their absorption intensities are low, which is consistent with our studies.

These results provide unambiguous evidence that impurities are integrally related to carrier generation. While we anticipate that the carrier concentration in the polymer increases with iron impurity concentration, we do not have a direct measurement of carrier concentration. However, the decrease in conductivity of the samples with increasing impurity content is more likely to be due to a decrease in carrier mobility and not a decrease in carrier concentration. In fact, the field effect mobility is observed to decrease with impurity content. Furthermore, the electron acceptor concentration, as determined by capacitance–voltage measurements, is observed to increase with impurity content. However, the acceptor concentration increases only 10-fold for a 100-fold increase in iron content and varies nonlinearly with the impurity concentration. The origin of this is yet unknown.

Conclusions

Octahedral Fe(III) complexes contribute to the origin of charge carriers in poly(thiophenes) prepared via oxidative coupling using ferric chloride. For the unannealed polymer of highest purity, the ratio of unpaired electron spins to thienyl groups is 1:1810. This value falls by a factor of 100 with increasing impurity concentration. Optical spectroscopy shows that even though the impurity concentration is high, the polymer can be considered to be in the low-doping-level regime.

The field effect carrier mobility in conjugated polymers of the polymers decreases with increasing levels of impurities, presumably due to scattering by ionized impurities. Given that mobilities decrease with increasing impurity levels, it is concluded that polymers with low impurity concentrations are more suitable for MIS-

(68) Horowitz, G.; Delannoy, P. *J. Appl. Phys.* **1991**, *70*, 469.
(69) Burroughes, J. H.; Friend, R. H. In ref 4, p 617.

FET applications. We find bulk conductivity decreases with increasing impurity levels most likely because the decrease in carrier mobility is larger than the increase in charge carrier concentration. C–V measurements reveal the formation of a relatively thick accumulation layer for the most chemically pure poly(3-alkylthiophene) upon application of a negative bias. The thickness of this layer is field dependent. The correlation of impurity with electrical properties is likely to be a general effect for π-conjugated polymers, although the origin of charge carriers/nature of impurities will vary depending on the synthetic route.

Acknowledgment. Financial support of this work by the National Sciences and Engineering Research Council of Canada, the National Research Council of Canada (Institute for Microstructural Sciences), and the Advanced Systems Institute of B.C. is gratefully acknowledged. The authors thank Drs. R. D. Sharma and C. H. W. Jones for assistance in Mössbauer spectroscopic analysis.

CM940351A